Arabian Journal for Science and Engineering (2019) 44:893–909
https://doi.org/10.1007/s13369-018-3353-5

RESEARCH ARTICLE - MECHANICAL ENGINEERING

Desirability-Based Multi-objective Optimization and Analysis of WEDM Characteristics of Aluminium (6082)/Tungsten Carbide Composites

K. Ravi Kumar[1] · **Nishasoms**[2]

Received: 22 November 2016 / Accepted: 17 May 2018 / Published online: 5 June 2018

Abstract
Wire electrical discharge machining is a broadly recognized unconventional machining process capable of accurately manufacturing rigid components with compound contours. The present study is to optimize the machining parameters of Al (6082)/tungsten carbide composite. Peak current, pulse-on time, pulse-off time, wire feed rate and tungsten carbide percentage were used as variables to study the material removal rate and surface roughness. Analysis of variance technique is used to study the effect on material removal rate and surface roughness. Material removal rate is primarily influenced by % tungsten carbide followed by peak current, pulse-off time, feed rate and pulse-on time, respectively. Surface roughness is highly influenced by peak current followed by % tungsten carbide, pulse-off time, pulse-on time and feed rate respectively. Scanning electron microscopic structures of the machined surfaces were characterized by the presence of hillocks, fine and deep craters, microcracks, protrusion, recast layers and debris. Desirability-based multi-objective optimization was employed to optimize the process parameters. The developed mathematical model has a good level of adequacy and can be used to predict the responses with minimum error. The experimental results along with the mathematical model and optimization will serve as a technical database for aerospace, automotive, military and commercial applications.

Keywords WEDM · Composites · Optimization · Desirability

1 Introduction

Metal matrix composites (MMCs) are important in modern industrial applications having both physical and mechanical properties including high strength, low weight and high wear resistance [1–3]. The use of conventional machining processes induces severe tool wear due to the abrasive nature of reinforcing particles, thus shortening the tool life [4,5]. WEDM is the best alternative for producing microscale parts with high-dimensional accuracy in terms of machining components of high hardness. WEDM is a thermal process in which the material gets eroded from the work piece by a series of sparks that occur between the work piece and the wire electrode separated by the dielectric fluid. WEDM process utilizes the electrical energy that generates a channel of plasma between the wire electrode and the work piece. The plasma gets converted into a high-temperature thermal energy that heats and melts the surface of the work piece material. The generated plasma channel breaks down when the pulsating current is turned off and the temperature gets reduced and the dielectric fluid flushes the molten particles from the machining zone in the form of debris [6]. Servo voltage, pulse-on time, pulse-off time, wire feed rate, reinforcement percentage, peak current, wire tension are the major process parameters influencing the surface roughness (SR) and kerf width in WEDM [7–9]. Machining depth plays a major role in inducing arching in EDM machining of TiB2p/Fe matrix composites [10]. Finest circularity in WEDM can be achieved at the moderate particle size, wire tension, pulse-on time and reinforcement size [11]. Material removal rate (MRR) depends on the coefficient of thermal expansion, amount of molten material, discharge channel radius and thermal properties [12]. Pragya Shandilya et al. [13] reported that servo voltage and pulse-off time are highly significant WEDM parameters in material removal of Al/SiC

✉ K. Ravi Kumar
ravik_krish@yahoo.com

Nishasoms
nishasoms@gmail.com

[1] Department of Mechanical Engineering, Dr. N.G.P. Institute of Technology, Coimbatore, India

[2] Department of Computer Science and Engineering, Sri Ramakrishna Institute of Technology, Coimbatore, India

composites. The weight fraction of reinforcement particles present in composites significantly influences the WEDM of aluminium composites [14]. Rozenek et al. [15] reported that the low electrical conductivity and thermal conductivity of aluminium composites leads to a decrease in MRR. Udaya et al. [16] stated that gap voltage is the most significant parameter affecting the MRR of composites. Sanjeev [17] used brass- and zinc-coated copper electrodes for machining high-speed steel and reported that the diffused wire electrode provided better performance in terms of cutting velocity and surface roughness. Yang et al. [18] observed some pores on the surface and three zones along the interior surface, namely the melting zone, heat-affected zone and unaffected zone after WEDM process of Al2024/SiC composites. Rajmohan et al. 19] found pock marks along the WEDM machined surface of duplex stainless steel that leads to an increase in surface roughness. Biing et al. [20] observed that thermal softening of the material at high temperature reduces the tensile strength of wire causing wire breakage which can be prevented by a low wire tension, high flushing rate and high wire speed. Amitesh and Jatinder [21] reported that high discharge energy leads to melting and subsequent formation of craters. Aniza et al. [22] observed that at low machine feed rate the machined surface is characterized by larger crater while machining titanium alloy using brass wire. Higher peak current and pulse-on time increase the pulse energy resulting in higher melting and evaporation of work piece leading to the formation of large size craters and cracks. The energy loss during WEDM is comprised of heat carried away by the debris due to conduction and heat loss due to convection and radiation [23,24]. Ravindranadh et al. [25] depicted that the high discharge heat generated during machining and subsequent rapid quenching induces the formation of spherical nodes near the heat-affected zone. Pramanik [26] found that the tool wear, tool breaking and recast layer are the main problems in electro-discharge machining of Al/Al_2O_3 composites. Sivaprakasam et al. [27] revealed that at insufficient flushing conditions and high gap pollution increases the MRR of composites. Khullar et al. [28] reported that selection of a wrong flushing mode resulted in inconsistent machining conditions and developed a non-dominating sorting genetic algorithm II (NSGA-II) to optimize the EDM parameters of steel. Pragadish et al. [29] fabricated a special attachment to rotate the tool while studying the EDM behaviour of steel. Arooj et al. [30] related globule formation with machining current and observed that globule diameter and inter-globule distance increased with increase in current.

Pragya and Jain [31,32] employed response surface methodology (RSM) and artificial neural network (ANN) techniques for predicting the WEDM parameters. Nihattosun et al. [33] employed Taguchi method to optimize the WEDM machining parameters. Rupesh and Jatinder [34] employed traditional utility optimization method in trim cut wire electrical discharge machining. Arindam et al. [35] employed RSM to achieve optimum responses of MRR while machining Al/Al_2O_3 composite. RSM was employed by Neeraj et al [36] to formulate a mathematical model to correlate the influence of process parameters on MRR and SR of high strength low alloy steel. Sidhu et al. [37] utilized lexicographic goal programming (LGP) approach and desirability function approach for predicting the material removal rate and tool wear rate of aluminium composites by EDM process. Rao et al. [38] utilized non-dominated sorting genetic algorithm (NSGA-II) to formulate the WEDM parameters of Al7075/SiCp composites. Derringer and Suich [39] described a multiple response method called desirability to optimize the multiple characteristics problems.

In the present work, an attempt has been made to optimize the WEDM parameters for machining aluminium (6082)/tungsten carbide composites. Pulse-off time, peak current, pulse-on time, WC percentage and wire feed are the variables used in this study to inspect the influence on MRR and SR of Al/WC composites. It is evident from the literature review that particles like SiC, B_4C, Al_2O_3, TiC, $ZrSiO_4$, fly ash were used as reinforcement particles in MMCs. Tungsten carbide particles having high hardness can also be used as reinforcement in aluminium matrix composites. Aluminium alloy (6082), a medium strength alloy with excellent corrosion resistance, wettability and machinability is one among the high strength alloy of 6000 series alloys. Al (6082) alloys are used in high-stress applications like trusses, bridges, cranes. Limited investigations were carried out to study the effect of WEDM parameters on aluminium composites and their influence on surface topography (SEM, atomic force microscopy (AFM)) and elemental composition. In addition to the surface morphology, it is essential to achieve the optimum WEDM parameters. The effect of machining parameters and their level of significance on MRR and SR were statistically evaluated using Analysis of Variance (ANOVA) and RSM techniques. The main objective of the paper is to develop mathematical models for correlating the influences of machining parameters, such as the peak current, pulse-on time, pulse-off time, wire feed rate and tungsten carbide percentage on the machining criteria, namely the MRR and SR. The material removal rate (MRR) generally indicates the degree of production, and surface roughness (Ra) indicates the dimensional accuracy and surface quality. It is necessary to balance these two parameters (MRR and SR) and achieve optimal WEDM machining by selecting appropriate machining variables. Optimal machining parameters of Al/WC composites were obtained by desirability-based multi-objective optimization technique. Desirability approach is based on the principle that when one of the responses of a process is not in the desired limits, then the overall desirability function is not acceptable. This method provides the most desirable response values

Table 1 Composition of aluminium 6082 alloy

Weight%	Al	Si	Fe	Cu	Mn	Cr	Mg	Zn	Ti	Others
6082	Balance	1.12	0.19	0.02	0.87	0.15	0.92	0.17	0.086	0.075

with better results. SEM and AFM were used to examine the effects of parameters on mechanism of MRR and SR. The experimental results and multi-objective optimization on WEDM of aluminium/tungsten carbide composites would be a database for various applications.

2 Materials and Measurements

2.1 Materials and Characteristics

Aluminium (Al 6082) shown in Table 1 is reinforced with tungsten carbide (2, 4, 6, 8 and 10%) and graphite (5%) by stir casting technique (Fig. 1). Aluminium alloy in the form of rod is melted at 800 °C in an electric resistance furnace and hexachloroethane compound was used for degassing. Preheating of tungsten carbide and graphite (Gr) was carried for one hour at 750 °C. The stirrer was then slowly lowered into the graphite crucible. The preheated WC and graphite particles were added into the melt at a stirring speed of 500 rpm. One weight per cent of magnesium was added with the melt to increase the wettability of reinforcement particles. The melt was then poured in the mould, and the composites were cut to 100 mm × 100 mm × 10 mm sizes (Fig. 2). In order to have a uniform standard surface finish along the surface, the cast composite specimens were ground using commercially used SiC 600-grit emery sheet. XRD analysis was employed to determine the element, structure, phase and purity of the samples. The XRD spectra of Al/WC composite samples are shown in Fig. 3. Peak values were observed by varying the 2θ angle from 10–90^{o} at a scanning rate of 10^{o} per minute. Presence of Al and WC is observed in XRD samples of composites. The presence of tungsten carbide particles increased with increase in WC. Microstructure of composites shown in Fig. 4 depicts that the tungsten carbide and graphite particles are evenly distributed in the aluminium matrix. The black dot indicates the presence of graphite, and the white one indicates the presence of tungsten carbide.

2.2 Measurement of MRR and SR

The WEDM tests were carried using ECOCUT make machine (Fig. 5). In this study 0.25 mm diameter diffused brass wire was used as cutting tool and deionized water as dielectric. Two input variables, namely the flushing pressure

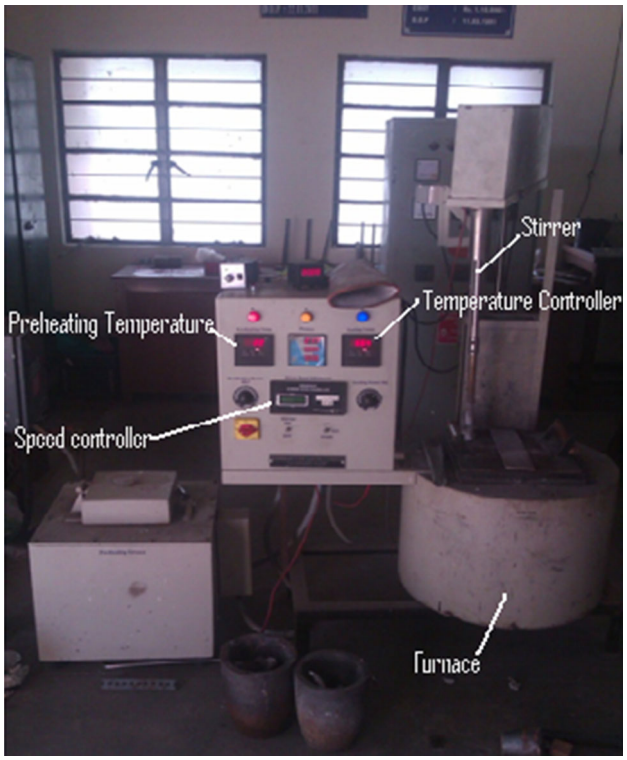

Fig. 1 Stir casting set-up

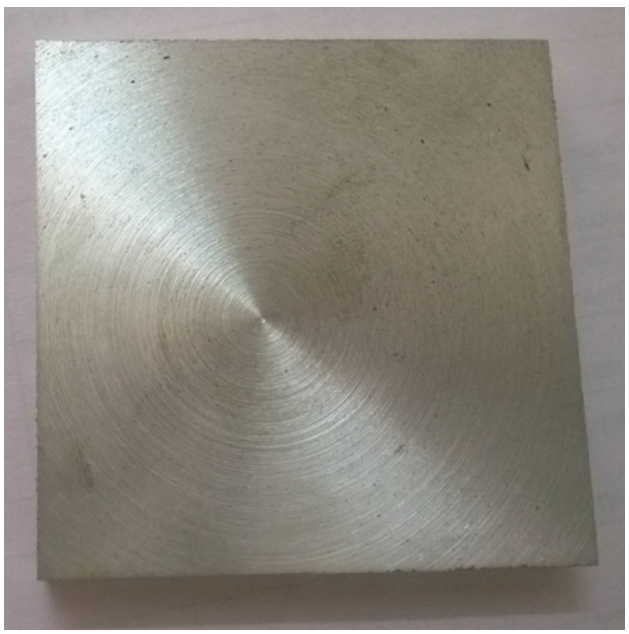

Fig. 2 Machined work piece

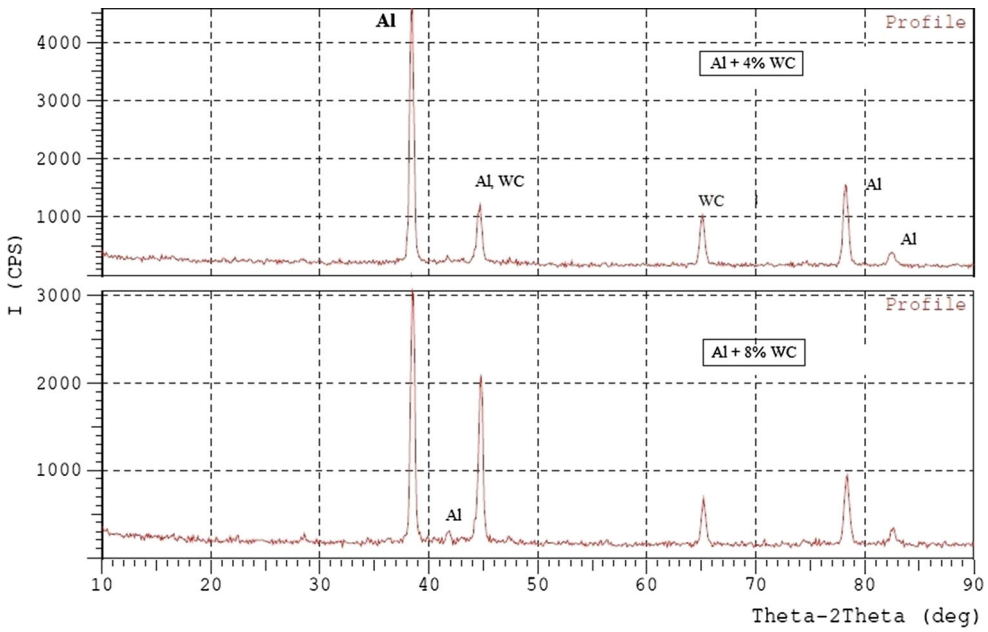

Fig. 3 XRD patterns of composite samples

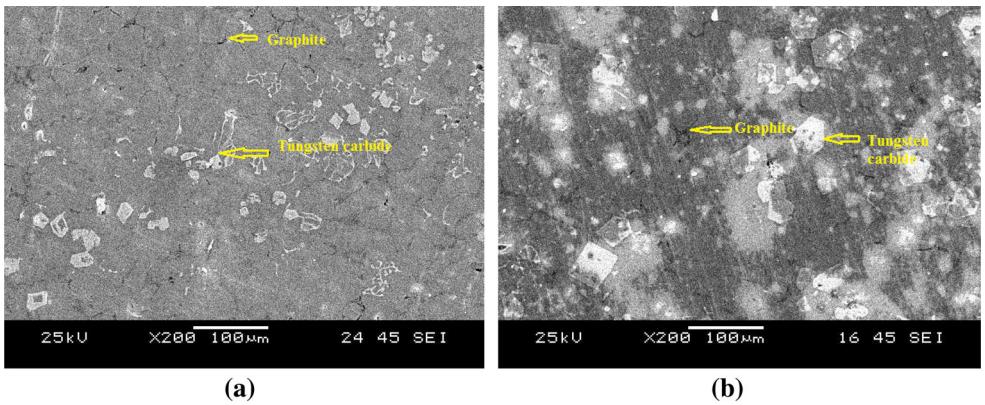

Fig. 4 SEM micrographs of the composite specimen. **a** 4% of tungsten carbide. **b** 8% of tungsten carbide

Fig. 5 Experimental set-up for WEDM

and servo voltage, were maintained constantly at 7 kg/cm^2 and 35 V, respectively. Five input process parameters namely the peak current (IP), pulse-on time (T_{ON}), pulse-off time (T_{OFF}), wire feed rate (WF) and tungsten carbide percentage (WC), were considered as input parameters in machining aluminium composites. The specimens were cut into 10 mm square as shown in Fig. 6. Material removal rate is calculated by using Eq. 1. An electronic weighing machine having accuracy 0.0001 g was used to find the weight loss. Density of the sample was observed using Archimedes principle, and machining time was observed using a stop watch. In order to minimize the measurement error, average value of three measurements for MRR and SR weight was used.

$$\text{MRR} = \text{Loss in weight}/(\text{density} \times \text{machining time}) \quad (1)$$

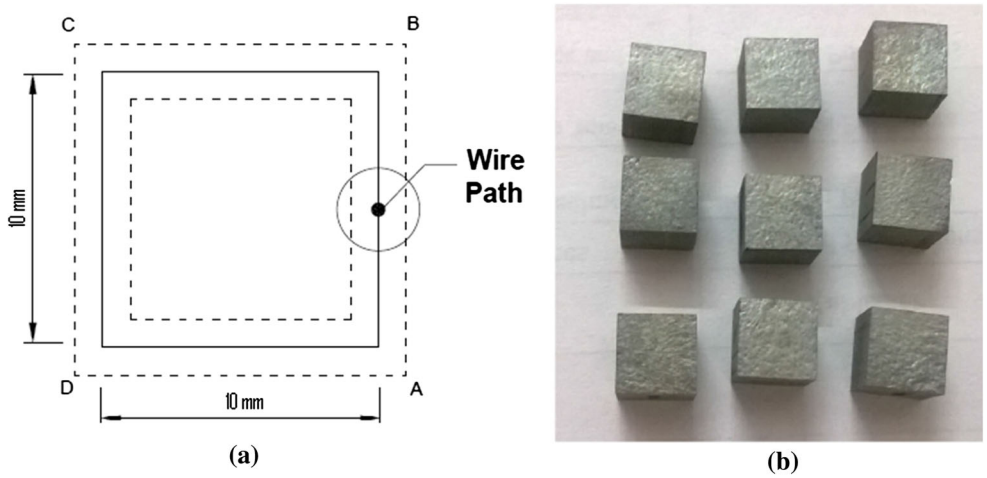

Fig. 6 **a** Rectangular profile cut on work piece. **b** Machined Al/WC samples

Table 2 Process variables and their levels

Parameters	Symbol	UNITS	Variable levels used				
			−2	−1	0	1	2
Peak current	IP	A	25	50	75	100	125
Pulse-on time	T_{ON}	S	4	8	12	16	20
Pulse-off time	T_{OFF}	S	2	4	6	8	10
Wire feed rate	WF	mm/min	10	20	30	40	50
Weight % of tungsten carbide	WC	%	2	4	6	8	10

3 Development of Response Surface Methodology

Response surface methodology approach is used to form the relation between the process parameters and their variables. A second-order polynomial response to represent the WEDM parameters, namely peak current, pulse-on time, pulse-off time, wire feed rate and % WC, is given in Eq. 2.

$$y = a_o + \sum_{i=1}^{n} a_i x_i + \sum_{i=1}^{n} a_{ii} x_i^2 + \sum_{i<j}^{n} a_{ij} x_i x_j + \varepsilon \qquad (2)$$

where y is the response surface corresponding to the input variable, x_i and x_j are the input variables, and x_i^2 and $x_i x_j$ are the quadratic and interaction terms of inputs. a_i, a_{ii} and a_{ij} indicate the unknown regression coefficients, and ε indicates the error.

Experiments were designed using Design–Expert-16 software to investigate the influence of parameters on MRR and SR. Five factors and five level of process parameters were used in the study (Table 2). A half-blocked central composite, face-centred alpha matrix, rotatable design with 32 set of experiments (Table 3) is used to optimize the experimental conditions. Experiments were conducted according to the run order in the experimental design matrix as shown in Table 3.

3.1 Analysis of Variance

After determining the significant coefficients, mathematical models developed by RSM for MRR and SR are given in Eqs. 3 and 4, respectively. Adequacy of the RSM model can be tested using ANOVA, and the responses are shown in Table 4. The model F value is 90.87 and 15.72 for MRR and SR, respectively. F value of the developed model exceeds the standard tabulated F value, and hence, the model is said to be sufficient. Analytical inspection of the developed response surface model of WEDM can be observed by the "lack of fit." If the model has lack of fit, it indicates that the model is inadequate. It can be observed from Table 4 that the models for MRR and SR are statistically significant. Also the coefficient of correlation "r" can be used to find the closeness of predicted and experimental values [35]. The square of coefficient of correlation (r^2) for MRR (0.963) and SR (0.932) indicates a high correlation between the experimental and forecast values.

$$\begin{aligned} \mathrm{MRR}\left(\frac{\mathrm{mm}^3}{\mathrm{min}}\right) &= 3.52 + (0.14 * \mathrm{IP}) + (0.057 * T_{\mathrm{ON}}) \\ &\quad - (0.071 * T_{\mathrm{OFF}}) + (0.064 * \mathrm{WF}) \\ &\quad - (0.21 * \mathrm{WC}) - 0.027 * T_{\mathrm{ON}} * T_{\mathrm{OFF}}) \\ &\quad - (0.040 * \mathrm{WF} * \mathrm{WC}) + \left(0.0097 * \mathrm{IP}^2\right) \end{aligned} \qquad (3)$$

Table 3 Experimental results for MRR and SR

Sl. Nos.	Peak current	Pulse-on time	Pulse-off time	Wire feed rate	Weight % of WC	Material removal rate (mm^3/min)	Surface roughness (μm)
1	−1	1	−1	−1	−1	3.720	6.731
2	−1	−1	−1	1	−1	3.729	6.131
3	−1	1	1	1	−1	3.728	6.354
4	0	0	0	−2	0	3.386	5.680
5	1	−1	1	−1	1	3.436	7.725
6	0	0	−2	0	0	3.718	8.223
7	0	−2	0	0	0	3.370	5.987
8	2	0	0	0	0	3.875	8.550
9	0	0	0	0	0	3.516	7.560
10	0	0	0	0	0	3.416	7.450
11	0	0	0	2	0	3.715	7.970
12	−1	−1	1	1	1	3.075	6.235
13	−2	0	0	0	0	3.218	4.586
14	0	0	2	0	0	3.346	6.300
15	1	1	1	−1	−1	3.752	6.625
16	0	0	0	0	2	3.090	8.753
17	1	1	−1	1	−1	4.077	8.835
18	1	1	−1	−1	1	3.563	9.147
19	−1	1	1	−1	1	3.116	5.525
20	1	1	1	1	1	3.443	8.623
21	0	0	0	0	0	3.520	7.413
22	0	0	0	0	0	3.580	7.683
23	0	0	0	0	0	3.536	7.806
24	1	−1	−1	1	1	3.456	8.364
25	−1	−1	−1	−1	1	3.119	7.478
26	0	2	0	0	0	3.625	8.156
27	−1	1	−1	1	1	3.376	8.261
28	0	0	0	0	0	3.536	6.898
29	1	−1	−1	−1	−1	3.782	6.588
30	1	−1	1	1	−1	3.890	7.180
31	−1	−1	1	−1	−1	3.417	5.254
32	0	0	0	0	−2	3.885	5.236

$$\begin{aligned}\text{SR}\,(\mu\text{m}) = {} & 7.17 + (0.79{*}\text{IP}) + (0.41{*}T_{\text{ON}}) \\ & - (0.49{*}T_{\text{OFF}}) + (0.40{*}\text{WF}) + (0.61{*}\text{WC}) \\ & + (0.058{*}\text{IP}*\text{WF}) - (0.10{*}T_{\text{ON}}*\text{WC}) \\ & - \left(0.012{*}T_{\text{ON}}^2\right)^{(4)}\end{aligned} \tag{4}$$

4 Results and Discussion

4.1 Influence of Parameters on Material Removal Rate

The effect of process parameters on MRR is shown in Fig. 8. It can be observed from equation [3] that % tungsten carbide primarily influences the MRR followed by peak current, pulse-off time, feed rate and pulse-on time, respectively. The high-temperature plasma energy generated in between the work piece and the wire electrode during machining vaporizes the work piece material and leads to the formation of tiny craters. The high-temperature energy distributed to electrodes is subjected to factors, namely dielectric material, discharge energy and flushing pressure of the dielectric medium. In WEDM process, the input energy is partially distributed to the dielectric medium and the remaining energy is distributed to the work piece and tool electrodes in different ratio known as fraction of energy. This fraction energy plays a vital role in WEDM process. The energy fraction distributed between the work piece and tool at variable input

Table 4 Analysis of variance (ANOVA) results

Source	Sum of squares	*df*	Mean square	*F* value	*p* value prob > *F*
Material removal rate					
Model	1.91	8	0.24	90.87	< 0.0001 significant
Residual	0.061	23	2.632 E-003		
Lack of fit	0.046	18	2.537 E-003	0.854	0.6389 not significant
Pure error	0.015	5	2.972 E-003		
Cor total	1.97	31			
SD	0.051	R-squared	0.9693		
Mean	3.53	Adj R-squared	0.9587		
C.V.%	0.13	Pred R-squared	0.9352		
PRESS	0.13	Adeq Precision	38.571		
Surface roughness					
Model	37.70	8	4.71	15.72	< 0.0001 significant
Residual	6.89	23	0.30		
Lack of fit	6.40	18	0.36	3.57	0.0818 not significant
Pure error	0.50	5	0.099		
Cor total	44.59	31			
SD	0.52	R-squared	0.9324		
Mean	6.94	Adj R-squared	0.9048		
C.V.%	6.69	Pred R-squared	0.8599		
PRESS	9.85	Adeq Precision	24.870		

parameters including the thermal conductivity of work piece and dielectric density affects the discharge current and the pulse duration. Difference in thermal properties between the aluminium alloy and the tungsten carbide particles leads to the thermal distortion of the composite specimen also influences the machining. It can be inferred from Fig. 7a that increase in feed rate increases the MRR, while MRR tends to decrease with increase in percentage tungsten carbide. Similar kind of results was reported by researchers in their studies. Nilesh and Brahmankar [12] reported that the MRR increased with increase in pulse-on time in aluminium/SiC composites. Singh and Garg [9] observed that increase in pulse-off time decreased the MRR of aluminium composites. Biing et al. [20] reported that the MRR of Aluminium/Al_2O_3 composites increased with increase in cutting speed. An increase in feed rate increased the wire tension, thereby leading to an easy and rapid escape of eroded material out of the spark gap. Decrease in spark gap results in rapid and large ionization of dielectric fluid, giving rise to more melting of work material and hence high MRR. Increase in percentage WC normally increases the hardness of the composites and hence decreases the MRR. Figure 7b shows the tendency of MRR to increase due to increase in peak current and pulse-on time. Increase in pulse-on time and peak current normally increases the number of electrons hitting the work surface, thus increasing the machining temperature and erosion of material from the work surface. Melting of materials and vaporization takes place at a faster rate at higher temperature along the work piece materials, thereby increasing the MRR. Shorter duration of pulse-on time leads to a decrease in discharge energy and hence a decrease in MRR of the composites. High pulse-on time melts the work piece and electrode by high thermal conduction; however, the vaporization of the melt electrode may be limited because of the high plasma pressures. Hard abrasive tungsten carbide particles present in the composites lead to the formation of built-up edges at high discharge energy which may also result in low MRR. During WEDM high discharge energy melts, a small portion of the matrix alloy and is evicted and flushed away by the dielectric medium. The remaining material left on the surface of the machined specimen solidifies and leads to the formation of a recast layer. Amitesh and Jatinder [21] reported that these high energy pulses vaporize a large amount of metal at the initial. A large percentage of work pieces are heated at the melting stage and redeposit on the surface as recast layer. The energy delivered along the work zone is used to heat the work piece, and the amount of heating is determined by the thermal conductivity, specific heat and density of the material [12]. The influence of pulse-on time and pulse-off time is depicted in Fig. 7c, keeping the peak current, feed rate and % WC as constant. Increase in pulse-off time decreases the temperature between successive sparks leading to a decrease in MRR. Increase in feed rate increases the wire tension and the forces on the wire electrode that leads an increase in MRR.

Influence in MRR with increase in parameters is shown in contour plot (Fig. 8). The red region indicates maximum

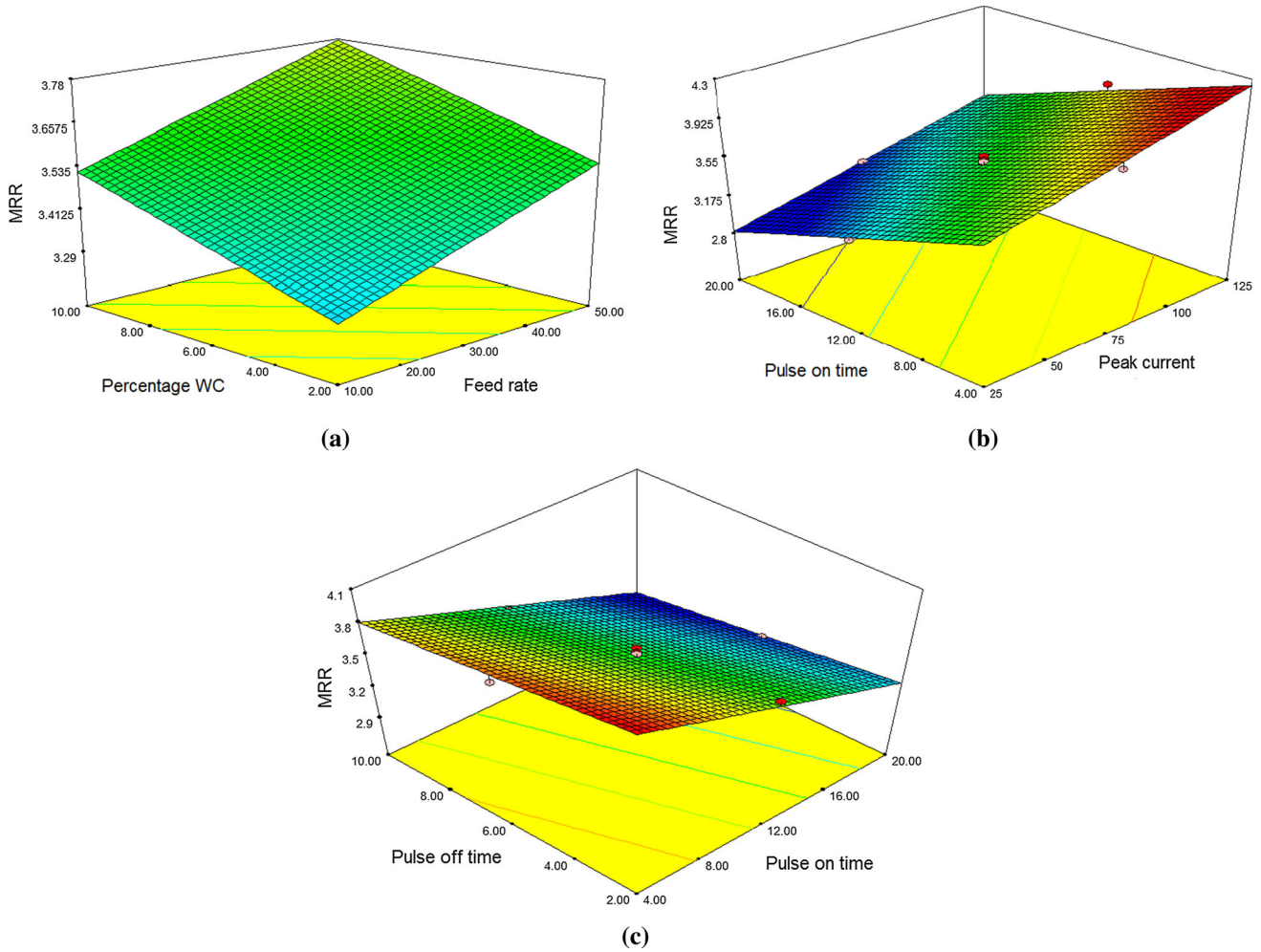

Fig. 7 3D surface place for material removal rate

MRR followed by green and blue regions indicating average and lower MRR, respectively.

4.2 Influence of Parameters on Surface Roughness

The interaction effect of parameters on SR is shown in Fig. 10. Influence of peak current and % WC is depicted in Fig. 9a, showing that the peak current and % WC increases the SR of composites. Pramanik [26] reported similar trend that increase in pulse-on time and peak current increases surface roughness of aluminium/Al_2O_3 composite. Rozenek et al. [15] reported that the cutting speed increases the SR of SiC and Al_2O_3reinforced composites. Low peak current decreased the discharge energy and hence reduces the SR favouring better surface condition [38]. At high pulse-on time the recast layers, large craters and thick debris are formed on the surface [21]. Increase in % tungsten carbide blocks the discharge passage creating a short circuit between the tool and work piece. These WC particles deposits along the surface of the work piece creating instability during machining and hence increase in surface roughness of the composites. According to Biing et al. [20], an increase in % reinforcement increases the protrusion of WC particles resulting in higher SR. An increase in pulse-on time increases the SR, while increase in pulse-off time decreases the SR (Fig. 9b). Longer pulse-on time results in larger MRR, thereby increasing the crater size on the surface and consequently increasing the surface roughness of composites [26]. Formation of craters is possible due to the high electrical conductivity and low melting temperature of aluminium matrix alloy. Higher peak current and longer pulse-on time increase the crater size and thereby increasing the surface roughness of the composite. It can be observed from Fig. 9c that SR increases with increase in feed. Higher pulse-off time favours the formation of fine craters indicating the formation of better surface finish. At higher peak current, the impact of discharge energy on the surface of work piece increases the erosion and subsequently increasing the surface roughness. Influence of parameters on SR is shown in contour plot (Fig. 10). The red region indi-

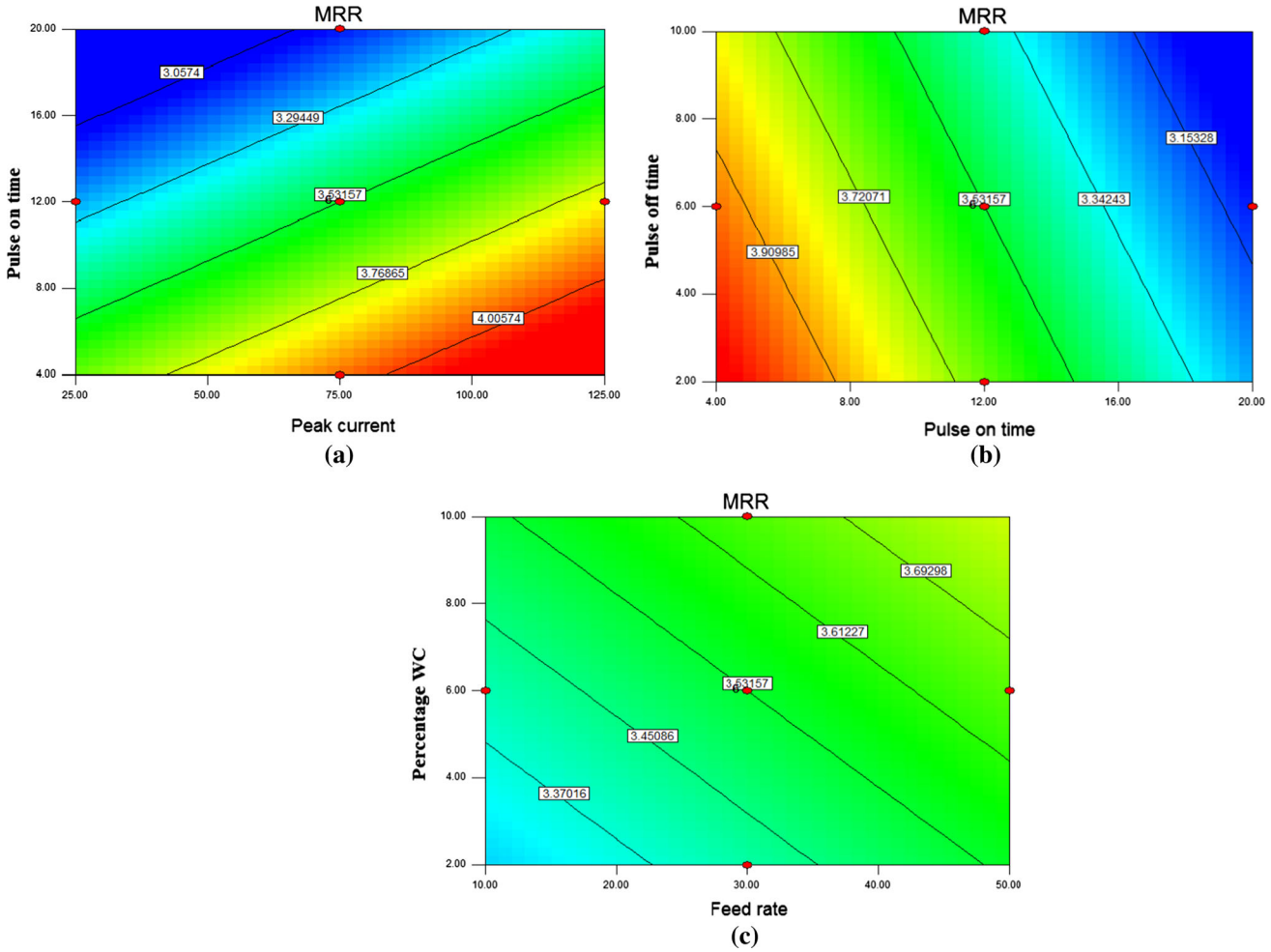

Fig. 8 2D contour plot for material removal rate

cates the maximum SR followed by green and blue regions indicating average and lower SR, respectively.

4.3 Scanning Electron Microscopy of the Machined Samples

SEM analysis was conducted on the surface of Al(6082)/WC/Gr composites to examine the mechanism of the machined surface. Microstructure of the machined surfaces for different input parameter settings is shown in Fig. 11. SEM of unreinforced aluminium alloy at low peak current and pulse-on time represents the absence of micro structural layers along the surface (Fig. 11a). Presence of graphite in the form of black spots is evidenced along the surface of the composites (Fig. 11b). Presence of debris is seen along the surface of the particles at minimum peak current values. Also the absence of recast layers, hillock and craters is found along the surfaces. This may be due to the bearing of graphite acting as an interface between the reinforcement and aluminium. However, at higher machining conditions the presence of liquid-like formation called as recast layers is observed along the surface of the composites in Fig. 11c–g. At this stage the impact of graphite particles has been reduced because of the high temperature developed at the machining zone. It can be observed from Fig. 8 that an increase in pulse-on time, peak current and feed rate increases the MRR. Increase in MRR can be correlated with the fact that at high machining conditions recast layers are formed due to the melting of resolidified aluminium alloy. The thickness of recast layer depends on the pulse energy and pulse duration which in turn is influenced by the input parameters. Presence of hillock and valleys can be observed from the micrograph surface of the composites. Minor hillocks and valleys are characterized with the lowest range values of input process parameters (Fig. 11a, b) which influence the surface roughness. SEM image of the cut surface at high input parameters shows moderate to large size hillocks and valleys. Presence of minor craters to deep craters and cracks (Fig. 11d–g) is evidenced on the surface of composites. The size of craters produced on the work piece surface is due to the discharge of energy influenced

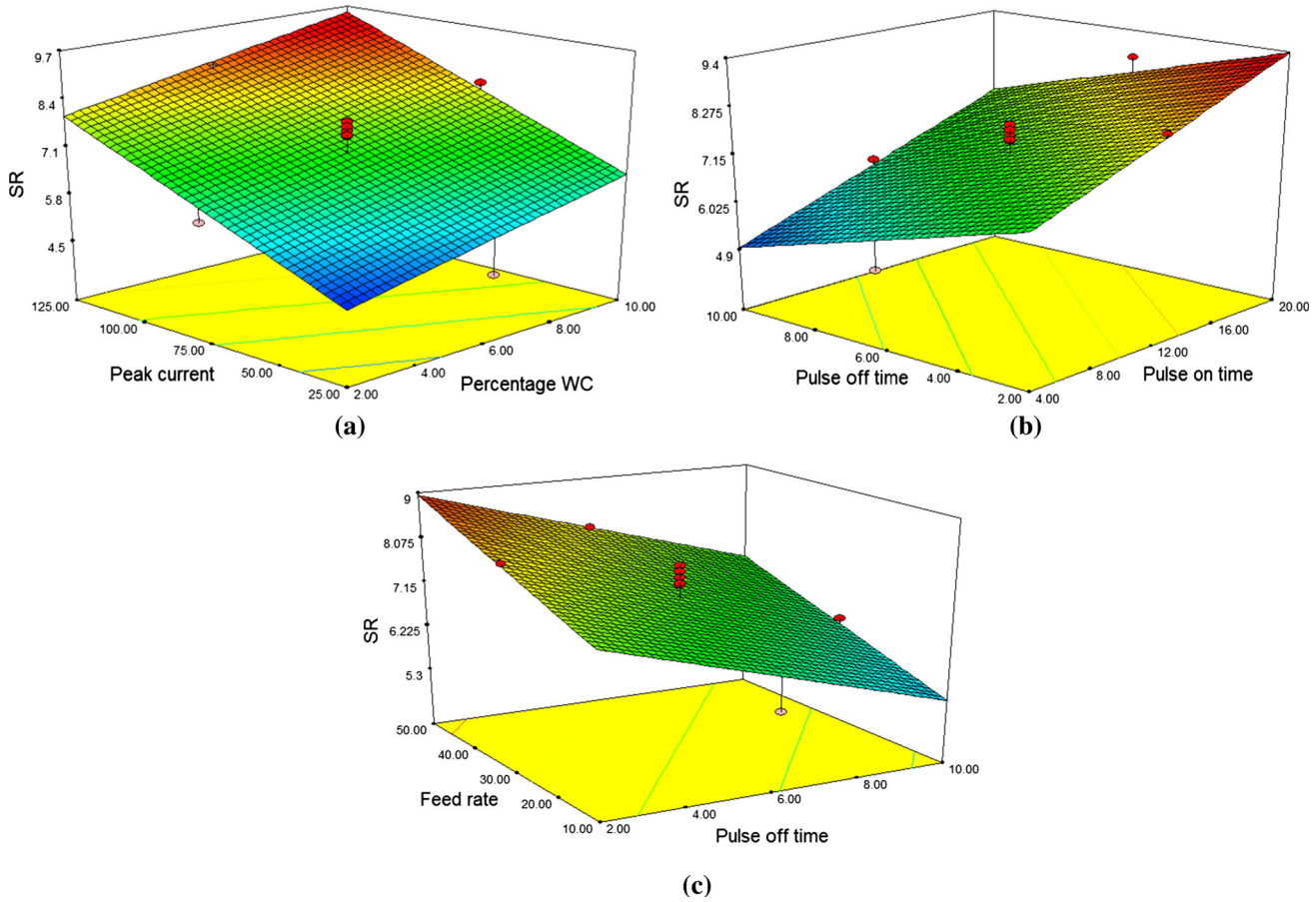

Fig. 9 3D surface plate for surface roughness

by the machining parameters. Craters are formed due to the pull-out and protrusion of particles along the machined surface [32]. Increase in peak current, pulse-on-time and low pulse-off time increases the residual stress of the composite, thereby increasing the material removal rate [37]. Increase in peak current increases the temperature leading to the melting of material at a high rate resulting in the formation of large craters [23]. An increase in peak current tends to increase the evaporation and cavitation of the dielectric material leading to the formation of smoke and bubbles that enables the formation of rough surface and even leads to the formation of cracks [30]. Presence of built-up edge layers is also observed along the surface of composites (Fig. 12h). This is due the increase in temperature resulting in deterioration of surface roughness. It can be observed from Fig. 11e, f that deep craters arise mainly due to the increase in pulse-on time, peak current and percentage reinforcement. These craters are formed due to pull-out of non-conductive particles (Fig. 11c) that inclines to the formation of deep holes on the machined surface. Porous layers due to air bubbles are observed on the surface (Fig. 11i), leading to an increase in SR. An increase in gap voltage increases the distance between the work piece and electrode, which leads to improper flushing and affects the surface roughness of the EDM [29]. Formation of these pores is due to the removal of the aluminium matrix from the graphite particles. An increase in pulse-on time increases the amount of heat transfer resulting in more metal removal and leaving the surface with large craters and cracks. Higher peak current increases the pulse energy, thereby increasing the melting and evaporation of work piece leading to the formation of large size craters and cracks. Formations of these cracks are due to the presence of tungsten carbide particles which reduces the softening of the material during machining. Increase in presence of tungsten carbide particles leads to the formation of craters is observed in Fig. 11g, i. This may be due to the resistance offered to erosion by the WC particles at different cutting condition. This confirms the RSM result that increase in WC particles decreases the MRR. Formation of large debris and deep holes/craters (Fig. 11h) on the surface of the composites is evidenced due to the high value of applied erosive power. To observe better resolution of the finished surface, AFM analysis was performed to observe the better resolution of the finished surface. It can be observed from Fig. 12a, b that the variation in crater height results in surface roughness of the composite specimen.

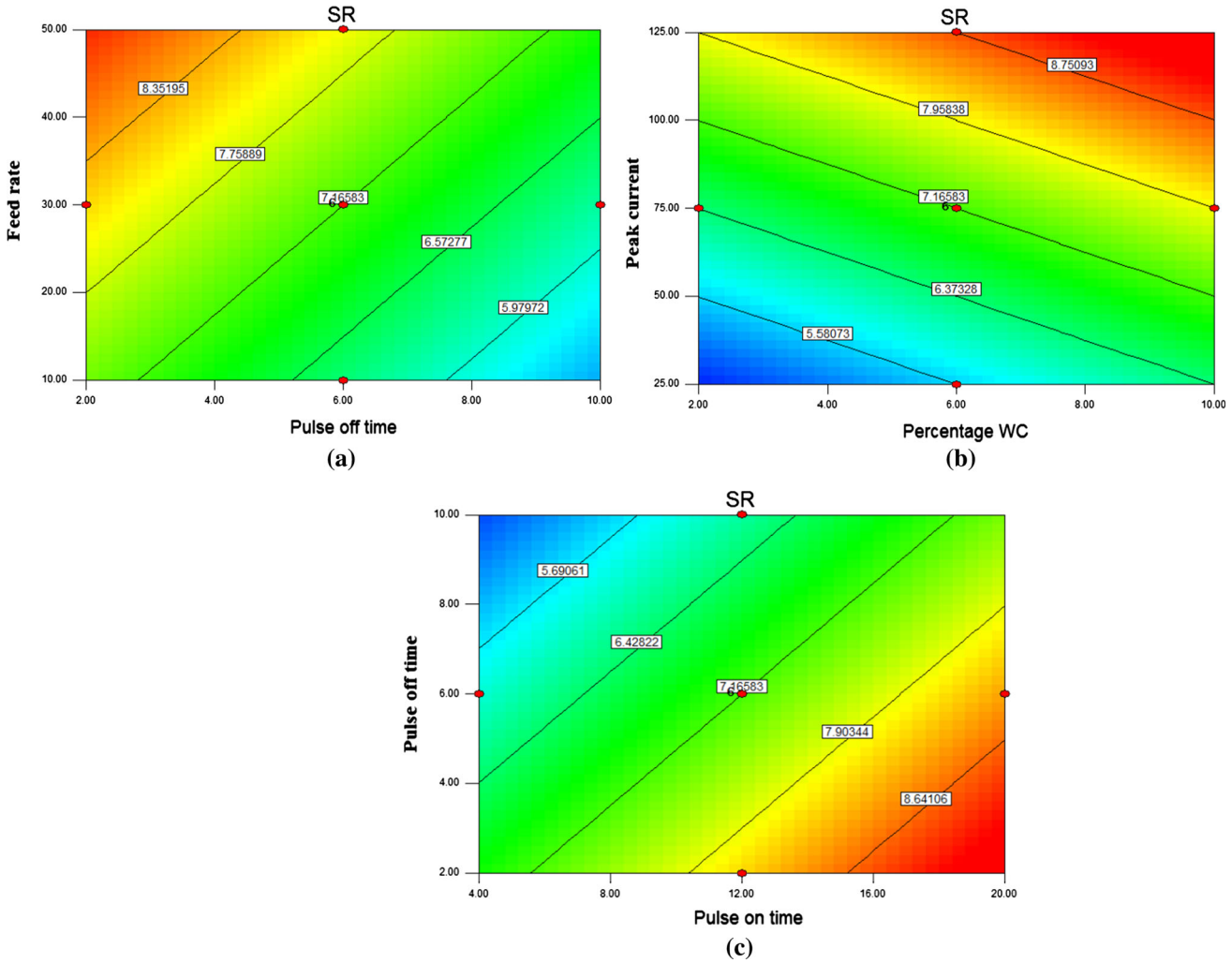

Fig. 10 2D contour plot for surface roughness

4.4 EDS Analysis

EDS spectra of the machined sample are shown in Fig. 13. Presence of oxide layers on the aluminium alloy (Fig. 13a) machined at low pulse-on time and peak current is 5.66% by weight. However, the percentage of oxides increased up to 23.46% (Fig. 13b) at higher peak current and pulse-on time. This leads to the formation of recast layers and hillocks as shown in Fig. 11. The machined sample contains 22.12% carbon and 23.46% oxides, indicating the migration of elements during machining. Presence of carbon layers was due to the addition of graphite particles and the presence of carbides present in the tungsten carbide.

4.5 Confirmation Tests

Confirmation experiments were carried out by assigning intermediate values to the process variables. Different intermediate values for pulse-on time (10 s, 14 s), pulse-off time (5 s, 7 s) and wire feed rate (45 mm/min) were assigned, and the responses are measured and recorded in Table 5. It can be observed from Table 5 that the maximum % error for MRR and SR was 8.25 and 6.38%, respectively, representing that the regression model is well within the acceptable range.

5 Multi-objective Optimization

Desirability method uses objective function $D(X)$, called the desirability function to transform an estimated response into a scale-free value (d_i) named as desirability [36]. The general approach of this technique is to first convert each response Y_i into a desirability function d_i that varies over the range $0 \leq d_i \leq 1$.

Desirability (d_i) of each response ranges from 0 to 1. The design variables are then chosen to maximize the overall desirability. An objective function D is given by equation (4).

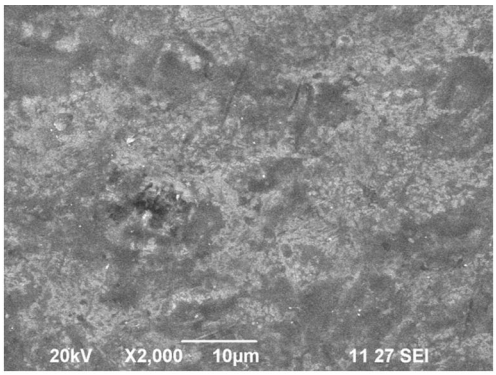

(a)

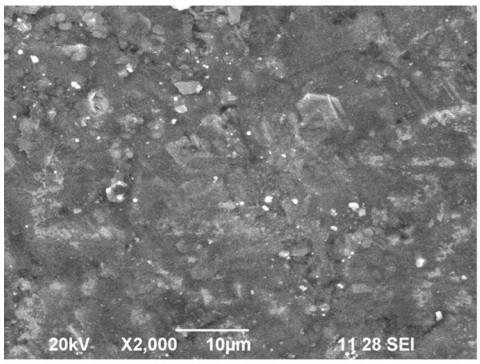

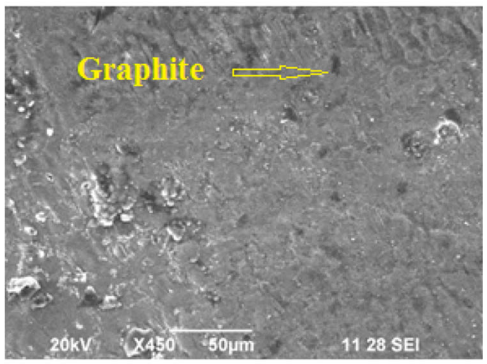

(b)

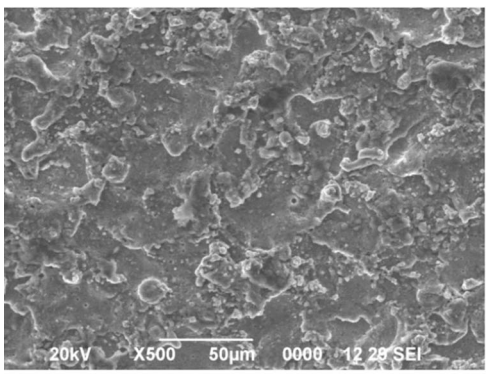

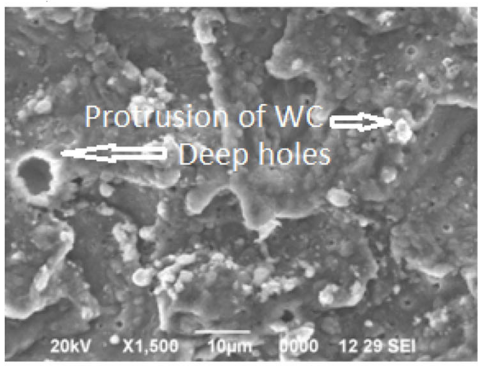

(c)

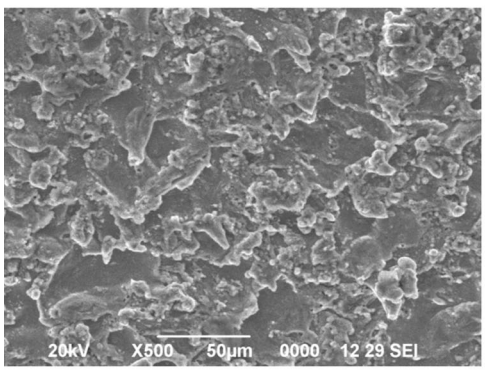

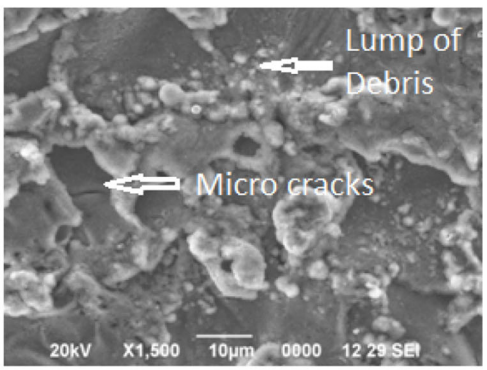

(d)

Fig. 11 SEM micrographs of the machined surface. **a** Peak current: 25, pulse-on time: 4, pulse-off time: 4, wire feed rate: 20, WC: 0%.**b** Peak current: 25, pulse-on time: 4, pulse-off time: 8, wire feed rate: 20, WC: 4%. **c** Peak current: 50, pulse-on time: 8, pulse-off time: 4, wire feed rate: 20, WC: 8%. **d** Peak current : 50, pulse-on time: 8, pulse-off time: 4, wire feed rate: 40, WC: 4%. **e** Peak current: 50, pulse-on time: 16, pulse-off time: 8, wire feed rate: 40, WC: 4%. **f** Peak current: 100, pulse-on time: 8, pulse-off time: 4, wire feed rate: 40, WC: 8%. **g** Peak current: 100, pulse-on time: 16, pulse-off time: 4, wire feed rate: 20, WC: 10%. **h** Peak current: 100, pulse-on time: 20, pulse-off time: 4, wire feed rate: 40, WC: 10%. **i** Peak current: 125, pulse-on time: 20, pulse-off time: 4, wire feed rate: 50, WC: 8%

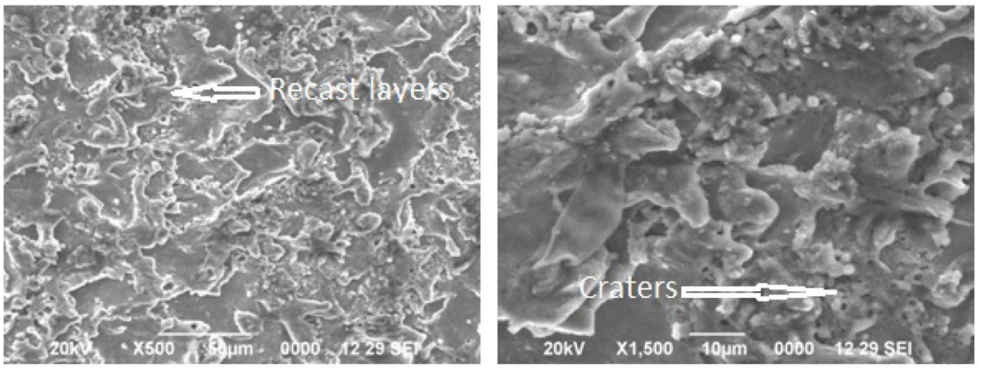

(e)

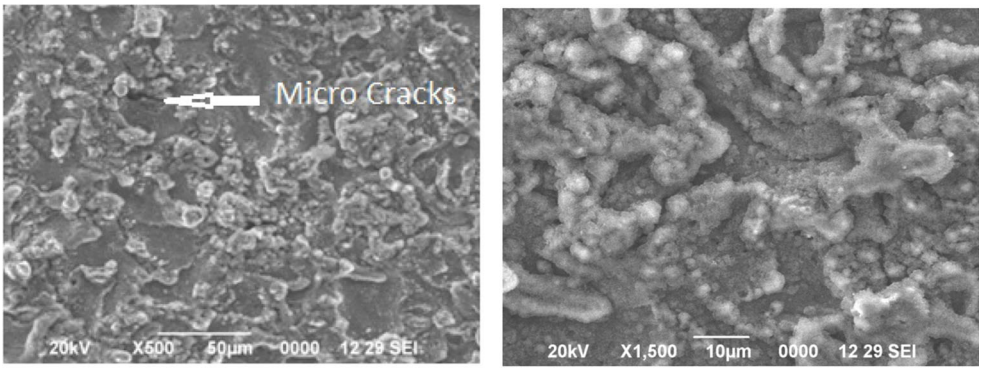

(f)

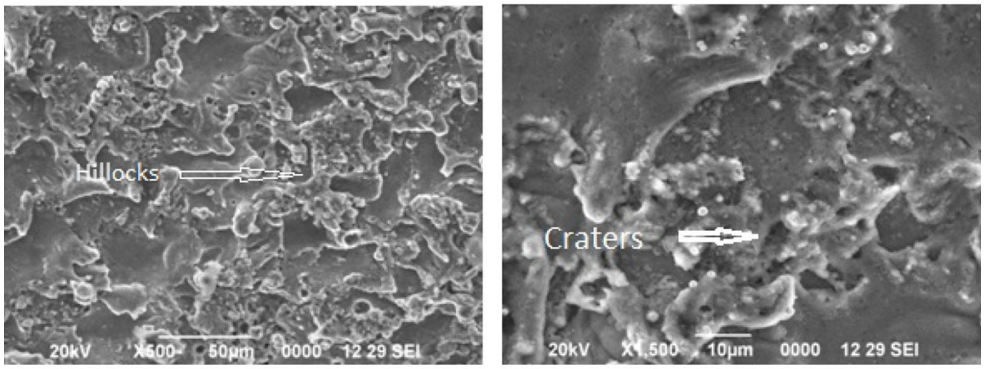

(g)

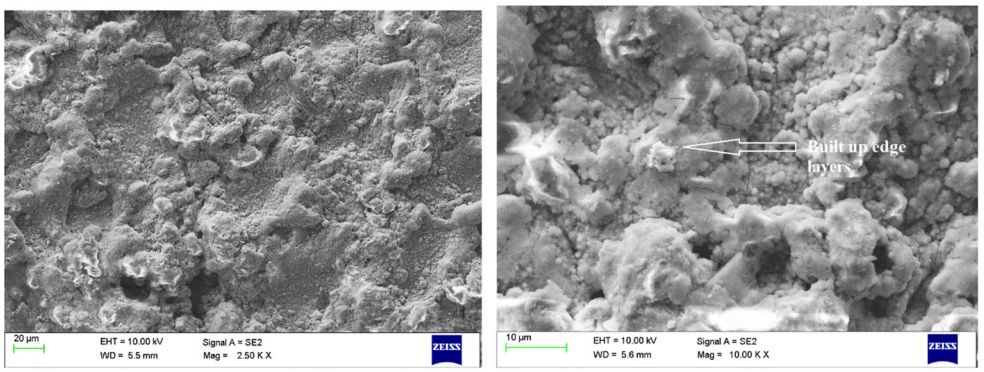

(h)

Fig. 11 continued

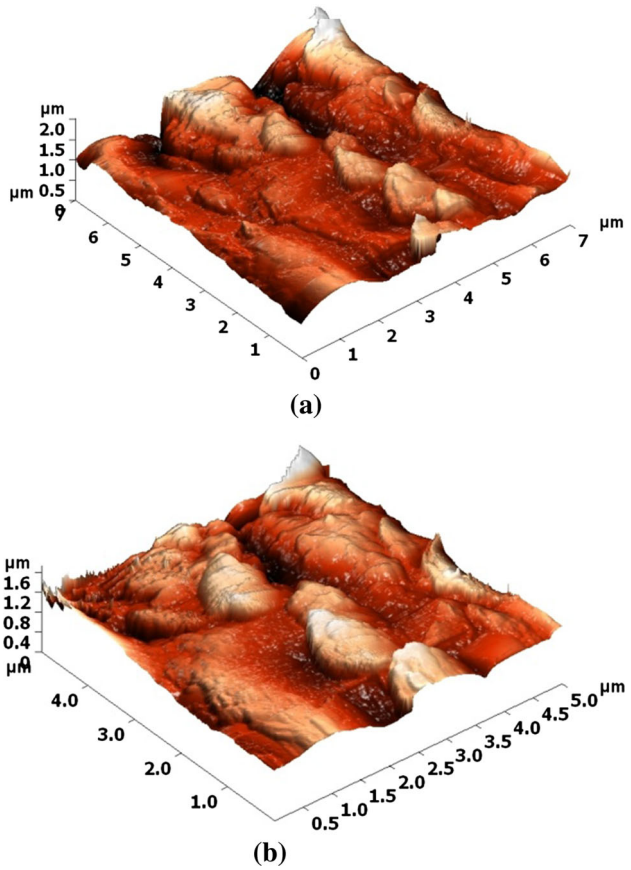

Fig. 12 Atomic force microscopy of confirmation test results. **a** Peak current: 50, pulse-on time: 14, pulse-off time: 8, wire feed rate: 40, WC: 4%. **b** Peak current: 50, pulse-on time: 10, pulse-off time: 4, wire feed rate: 20, WC: 4%)

$$D = (d_1 X d_2 X \ldots\ldots d_n)^{1/n} = \left(\prod_{i=1}^{n} d_i\right)^{1/n} \quad (5)$$

Design–Expert software is used to evaluate the desirability value. The optimality solution is to maximize the MRR and minimize the SR. The optimum values of input parameters and the output characteristics are given in Table 6. The constraints of process parameters during multi-objective optimization of WEDM play an important role. Weights normally give an added emphasis to upper or lower bounds and target value. The desirability varies from 0 to 1 in linear fashion for a weight of 1. In case the weight is greater than 1 (maximum weight is 10), then it gives more emphasis to goals while weights less than 1 (minimum weight is 0.1) give less emphasis to goals. In order to fine tune the optimization, both lower and upper weights are assigned as 1. Importance is a tool for changing the relative priorities to achieve the goals. To emphasize one variable over the rest, higher importance has to be assigned for that variable. Design–Expert offers five levels of importance ranging from 1 to 5. In this study to have equal emphasis to the parameters and variables, a medium setting of 3 was used so that none of the target is favoured over the other. The process parameters were allowed to vary from lower limit to higher limit. The overall desirability function of the responses is shown in the bar graph and ramp graph (Figs. 14, 15). Depending upon the closeness of the response towards output, the desirability varies from 0 to 1. The desirability value for surface roughness and material removal rate is 0.93 and 0.76 (Fig. 14). The near optimal region had an overall desirability value of 0.845 indicating the optimized vale closer to the target. The optimum parameter set for the current study is peak current: 116.81 Amps, pulse-on time:

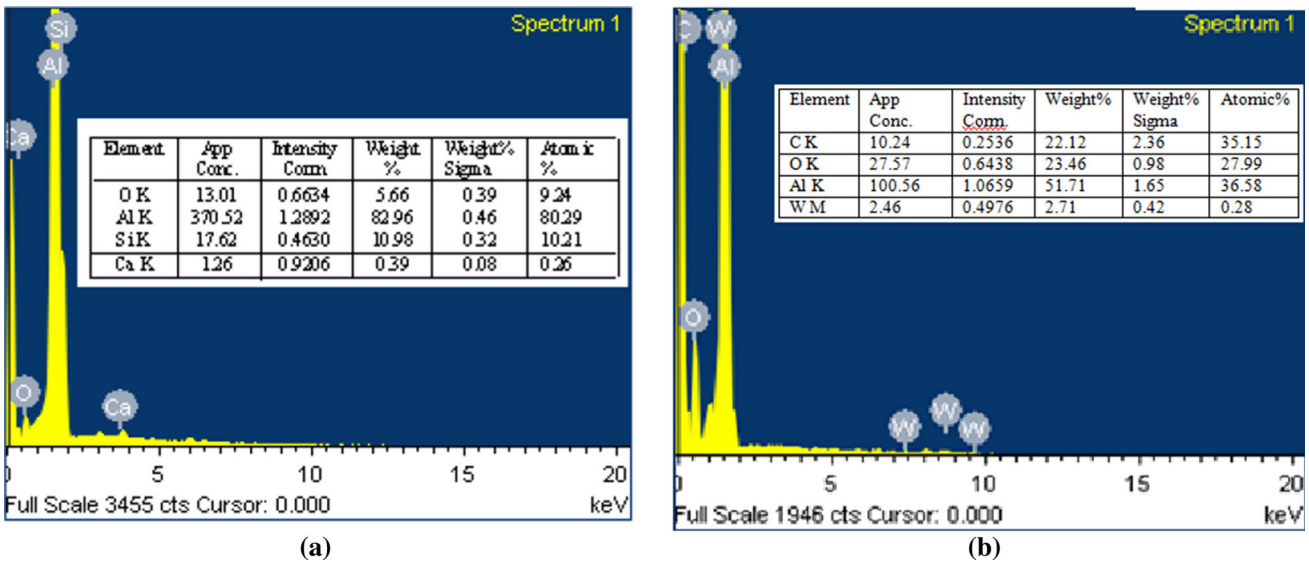

Fig. 13 EDS pattern of composites after WEDM test. **a** Peak current: 25, pulse-on time: 4, **b** peak current: 50, pulse-on time: 8, pulse-off time: 4, wire feed rate: 20, WC: 0%; pulse-off time: 4, wire feed rate: 40, WC: 4%

Table 5 Confirmation of WEDM test results

Sl. Nos.	Process parameters					Actual		Regression model		% Error	
	IP	T_{ON}	T_{OFF}	WF	WC	MRR	SR	MRR	SR	MRR	SR
1	50	10	4	20	4	3.418	5.870	3.524	5.661	3.13	3.58
2	125	12	7	30	6	3.987	7.995	3.803	8.505	4.61	6.38
3	100	16	8	45	8	3.678	9.623	3.454	9.065	6.06	5.80
4	50	14	8	40	4	3.976	6.237	3.647	5.874	8.25	5.82
5	50	8	5	40	8	3.295	7.458	3.168	7.255	3.84	2.72
Average										5.178	4.86

Table 6 Range of parameters and responses for desirability

Sl. Nos.	Process parameter	Goal	Lower limit	Upper limit	Lower weight	Upper weight	Importance	Optimum values
1	Peak current	In range	25	125	1	1	3	116.81
2	Pulse-on time	In range	4	20	1	1	3	4
3	Pulse-off time	In range	2	10	1	1	3	9.99
4	Wire feed rate	In range	10	50	1	1	3	14.77
5	Weight % of WC	In range	2	10	1	1	3	2.05
6	MRR (mm^3/min)	Maximize	3.075	4.0768	1	1	3	3.843
8	SR (μm)	Minimize	4.586	9.147	1	1	3	4.899

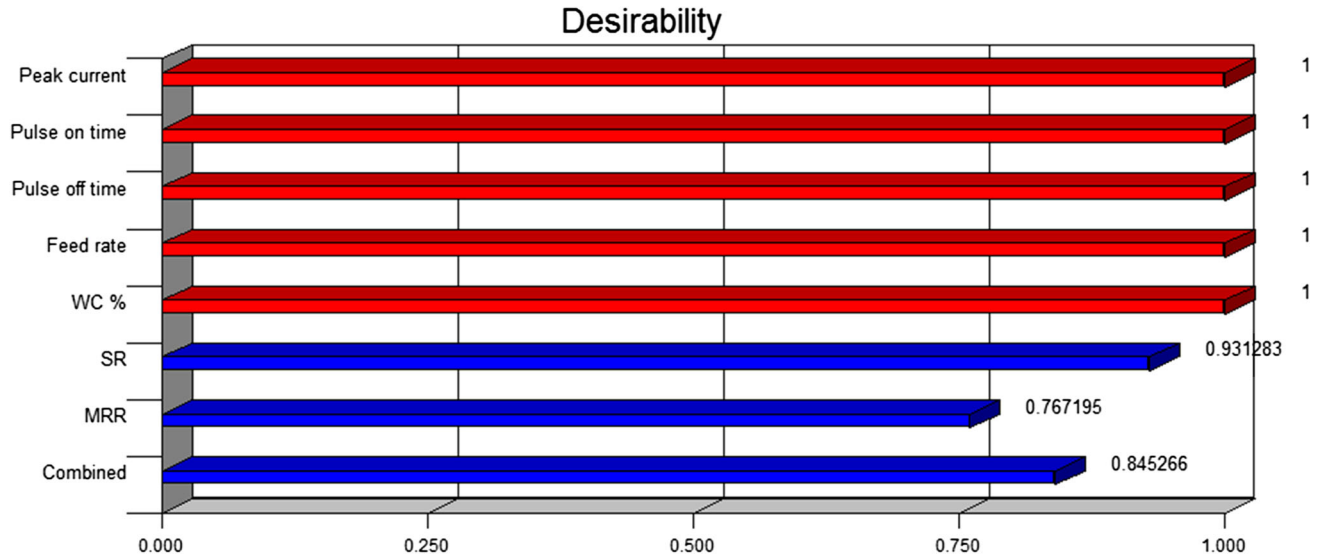

Fig. 14 Bar graph for desirability

4 s, pulse-off time: 9.99 s, feed rate: 14.77 mm/min and percentage WC: 2.05% for maximizing the MRR and minimizing the SR. Better combination of MRR and SR can be observed at lower %of WC, pulse-on time, feed rate, higher pulse-off time and moderate peak current.

6 Conclusions

The influence of process parameters on MRR and SR of aluminium (6082)/WC/graphite composites was investigated.

- Response surface methodology (RSM) approach is used to determine the relation between the parameters and their responses.
- A mathematical model was developed to obtain the MRR and SR of aluminium (6082)/WC/graphite composites. ANOVA technique was employed to test the adequacy of the proposed model.
- MRR of composite is primarily influenced % tungsten carbide followed by peak current, pulse-off time, feed rate and pulse-on time, respectively.

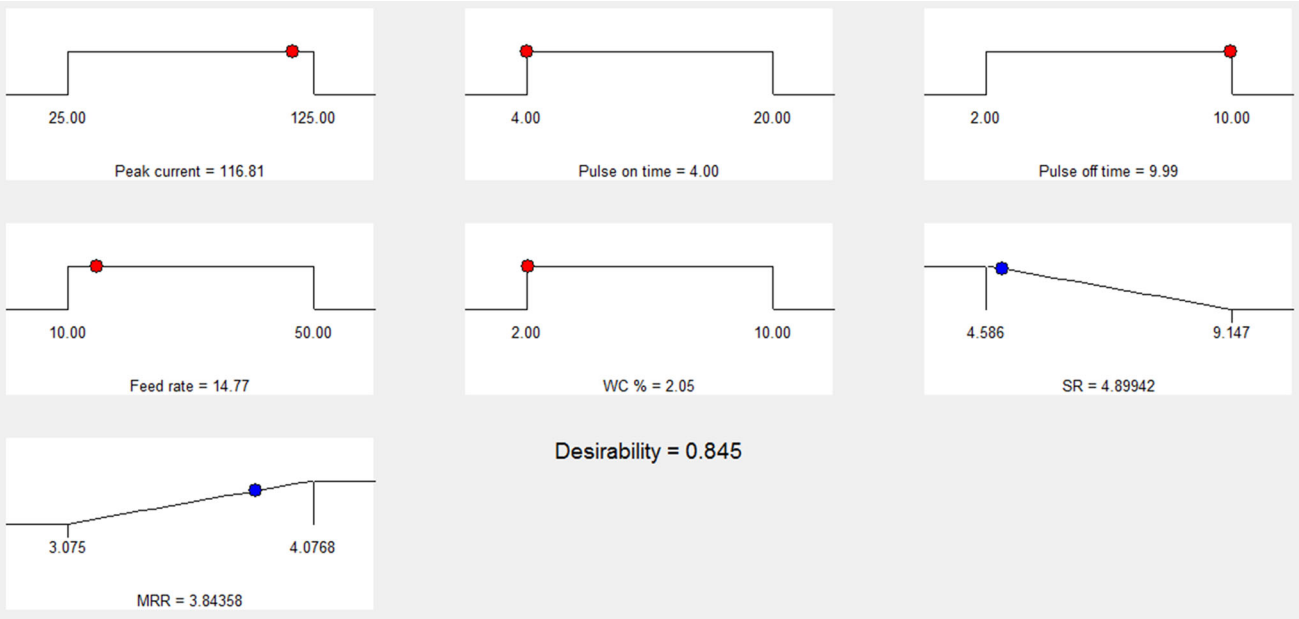

Fig. 15 Ramp graph for desirability

- SR influenced by peak current followed by % tungsten carbide, pulse-off time, pulse-off time and wire feed rate, respectively.
- Increased energy per spark, high current pulse duration and decreasing pulse-off time increase the thickness of the recast layer that influences the SR and MRR of the composites.
- EDS revealed that the percentage of oxides increased at higher peak current and pulse-on time leading to the formation of recast layers in composites.
- SEM of unreinforced aluminium alloy at low peak current and pulse-on time represents the absence of microstructural layers along the surface.
- At higher machining conditions the presence of liquid-like formation called as recast layers is observed along the surface of the composites.
- Minor hillocks and valleys are observed along surface of the composites at lowest range values of input process parameters.
- Deep craters due to pull-out of non-conductive particles arise mainly at higher pulse-on time, peak current and percentage reinforcement.
- Low variation in crater height of the surfaces results in lower surface roughness of the composite specimen.
- At very high temperature, porous layers were formed on the composite due to the formation of air bubbles thereby increasing the surface roughness.
- Atomic force microscopy revealed that variation in crater height results in surface roughness of the composite specimen.
- Desirability-based multi-objective optimization technique was employed to optimize the process parameters. The optimum parameters for the current study are peak current 116.81A, pulse-on time 4 s, pulse-off time 9.99 s, feed rate 14.77 mm/min and WC 2.05% for maximizing the MRR and minimizing the SR. The optimized parameters are in line with the RSM values.

References

1. Miracle, D.B.: Metal matrix composites-from science to technological significance. Compos. Sci. Technol. **65**, 2526–2540 (2005)
2. Rosso, M.: Ceramic and metal matrix composites: routes and properties. J. Mater. Process. Technol. **175**, 364–375 (2006)
3. Ravi Kumar, K.; Mohanasundaram, K.M.; Arumaikkannu, G.; Subramanian, R.: Analysis of parameters influencing wear and frictional behavior of aluminum-fly ash composites. Tribol. Trans. **55**(2012), 723–729 (2012)
4. Yan, B.H.; Wang, C.C.: Machinability of SiC particle reinforced aluminum alloy composite material. J. Jpn. Inst. Light Met. **43**(4), 187–192 (1993)
5. Monaghan, J.M.; Reilly, P.O.: The drilling of an Al/SiC metal matrix composite. J. Mater. Process. Technol. **33**(4), 469–480 (1992)
6. Ho, K.H.; Newman, S.T.; Rahimifard, S.; Allen, R.D.: State of art in wire electrical discharge machining (WEDM). Int. J. Mach. Tools Manuf. **44**, 1247–1259 (2004)
7. Shandilya, P.; Jain, P.K.; Jain, N.K.: Parametric optimization during wire electrical discharge machining using response surface methodology. Procedia Eng. **38**, 2371–2377 (2012)
8. Sah, P.; Tarafd, D.; Pal, S.K.: Modelling of wire electro-discharge machining of TiC/Fe in situ metal matrix composite using normalized RGFN with enhanced *K*-means clustering technique. Int. J. Adv. Manuf. Technol. **43**(1), 107–116 (2009)

9. Singh, H.; Garg, R.: Effects of process parameters on material removal rate in WEDM. J. Achieve. Mater. Manuf. Eng. **32**(1), 70–74 (2009)
10. Pandey, A.B.; Brahmankar, P.K.: A method to predict possibility of arcing in EDM of TiB2p reinforced ferrous matrix composite. Int. J. Adv. Manuf. Technol. **86**(9–12), 2837–2849 (2016)
11. Pramanik, A.,; Islam, M.N.; Boswell, B.; Basak, A.K.; Dong, Y.; Littlefair, G.: Accuracy and finish during wire electric discharge machining of metal matrix composites for different reinforcement size and machining conditions. Proc. IMechE B J. Eng. Manuf. (2016). https://doi.org/10.1177/0954405416662079
12. Patil, N.G.; Brahmankar, P.K.: Determination of material removal rate in wire electro-discharge machining of metal matrix composites using dimensional analysis. Int. J. Adv. Manuf. Technol. **51**, 599–610 (2010)
13. Shandilya, P.; Jain, P.K.; Jain, N.K.: Modelling and process optimisation for wire electric discharge machining of metal matrix composites. Int. J. Mach. Mach. Mater. **18**(4), 377–391 (2016)
14. Dey, A.; Pandey, K.M.: Wire electrical discharge machining characteristics of AA6061/ cenosphere as-cast aluminium matrix composites. Mater. Manuf. Process. (2017). https://doi.org/10.1080/10426914.2017.1388517
15. Rozenek, M.; Kozak, J.; Dabrowski, L.; Lubkowski, K.: Electrical discharge machining characteristics of metal matrix composites. J. Mater. Process. Technol. **109**, 367–370 (2001)
16. UdayaPrakash, J.; Moorthy, T.V.; Peter, M.: Experimental investigations on machinability of aluminium alloy (A413)/fly ash/B_4C hybrid composites using wire EDM. Procedia Eng. **64**, 1344–1353 (2013)
17. Garg, S.K.R.; Manna, A.; Jain, A.: Multi-objective optimization of machining characteristics during wire electrical discharge machining of Al/ZrO_2 particulate reinforced metal matrix composite. J. Eng. Res. **1**(3), 145–160 (2013)
18. Yang, W.-S.; Chen, G.-Q.; Wu, P.; Hussain, M.; Song, J.-B.; Dong, R.-H.; Wu, G.-H.: Electrical discharge machining of Al2024-65 vol% SiC composites. Acta Metall. Sin. **30**(5), 447–455 (2017)
19. Rajmohan, K.; Senthil Kumar, K.: Experimental investigation and prediction of optimum process parameters of micro-wire-cut EDM of 2205 DSS. Int. J. Adv. Manuf. Technol. **93**(1–4), 187–201 (2017)
20. Yan, B.H.; Tsai, H.C.; Huang, F.Y.; Lee, L.C.: Examination of wire electrical discharge machining of Al_2O_3p/6061Al composites. Int. J. Mach. Tools Manuf. **45**(3), 251–259 (2005)
21. Goswami, A.; Kumar, J.: Investigation of surface integrity, material removal rate and wire wear ratio for WEDM of Nimonic 80A alloy using GRA and Taguchi method. Eng. Sci. Technol. **17**(4), 173–184 (2014)
22. Aliasa, A.; Abdullaha, B.; Abbasa, N.M.: WEDM: influence of machine feed rate in machining titanium ti-6al-4v using brass wire and constant current (4A). Procedia Eng. **41**, 1812–1817 (2012)
23. Sharma, A.; Gargand, M.P.; Goyal, K.K.: Prediction of optimal conditions for WEDM of Al 6063/$ZrSiO_4$ (p) MMC. Procedia Mater. Sci. **6**, 1024–1033 (2014)
24. Bobbili, R.; Madhu, V.; Gogia, A.K.: Modelling and analysis of material removal rate and surface roughness in wire-cut EDM of armour materials. Eng. Sci. Technol. Int. J. **18**, 664–668 (2015)
25. Bobbili, R.; Madhu, V.; Gogia, A.K.: An experimental investigation of wire electrical discharge machining of hot-pressed boron carbide. Def. Technol. **11**(4), 344–349 (2015)
26. Pramanik, A.: Developments in the non-traditional machining of particle reinforced metal matrix composites. Int. J. Mach. Tools Manuf. **86**, 44–61 (2014)
27. Sivaprakasam, P.; Hariharan, P.; Gowri, S.: Modeling and analysis of micro-WEDM process of titanium alloy (Ti/6Al/4V) using response surface approach. Eng. Sci. Technol. **17**, 227–235 (2014)
28. Khullar, V.R.; Sharma, N.; Kishore, S.; Sharma, R.: RSM- and NSGA-II-based multiple performance characteristics optimization of EDM parameters for AISI 5160. Arab. J. Sci. Eng. **42**(5), 1917–1928 (2017)
29. Pragadish, N.; Pradeep Kumar, K.: Optimization of dry EDM process parameters using grey relational analysis. Arab. J. Sci. Eng. **41**(11), 4383–4390 (2016)
30. Arooj, S.; Shah, M.; Sadiq, S.; Jaffery, S.H.I.; Khushnood, S.: Effect of current in the EDM machining of aluminum 6061 T6 and its effect on the surface morphology. Arab. J. Sci. Eng. **39**(5), 4187–4199 (2014)
31. Pragya, S.; Jain, P.K.; Jain, N.K.: Prediction of surface roughness during wire electrical discharge machining of SiC p/6061 Al metal matrix composite. Int. J. Ind. Syst. Eng. **12**(3), 301–315 (2012)
32. Shandilya, P.; Jain, P.K.; Jain, N.K.: RSM and ANN modeling approaches for predicting average cutting speed during WEDM of SiCp/6061 Al MMC. Procedia Eng **64**, 767–774 (2013)
33. Tosun, N.; Cogun, C.; Tosun, G.: A study on kerf and material removal rate in wire electrical discharge machining based on taguchi method. J. Mater. Process. Technol. **152**(3), 316–322 (2004)
34. Chalisgaonkar, R.; Kumar, J.: Multi-response optimization and modeling of trim cut WEDM operation of commercially pure titanium (CP Ti) considering multiple user's preferences. Eng. Sci. Technol. Int. J. **18**, 125–134 (2015)
35. Ghosal, A.; Manna, A.: Response surface method based optimization of ytterbium fiber laser parameter during machining of Al/Al_2O_3-MMC. Opt. Laser Technol. **46**, 67–76 (2013)
36. Sharma, N.; Khanna, R.; Gupta, R.: Multi quality characteristics of WEDM process parameters with RSM. Eng. Sci. Technol. **64**, 710–719 (2013)
37. Sidhu, S.S.; Yazdani, M.: Comparative analysis of MCDM techniques for EDM of SiC/A359 composite. Arab. J. Sci. Eng **43**(3), 1093–1102 (2018)
38. Rao, T.B.; Gopala Krishna, A.: Selection of optimal process parameters in WEDM while machining Al7075/SiCp metal matrix composites. Int. J. Adv. Manuf. Tech. **73**(1–4), 299–314 (2014)
39. Derringer, G.; Suich, R.: Simultaneous optimization of several response variables. J Qual. Technol. **12**(4), 214–219 (1980)
40. Montgomery, D.C.: Design and Analysis of Experiments, 5th edn. Wiley, New Delhi (2004)
41. Ravi Kumar, K.; Sreebalaji, V.S.: Desirability based multi objective optimization of abrasive wear and frictional behaviour of aluminium (Al/3.25Cu/8.5Si)/ fly ash composites. Tribol. Mater. Surf. Interfaces **9**, 128–136 (2015)